Communications in Physics, Vol. 30, No. 2 (2020), pp. 181-187
DOI:10.15625/0868-3166/30/2/13819

DETECTION OF LUMINESCENCE CENTERS IN COLLOIDAL $Cd_{0.3}Zn_{0.7}S$ NANOCRYSTALS BY SYNCHRONOUS LUMINESCENCE SPECTROSCOPY

PHI VAN THANG[1], HO VAN TUYEN[2], VU XUAN QUANG[2], NGUYEN THI THUY LIEU[3], NGUYEN TRONG THANH[4,†] AND NGUYEN XUAN NGHIA[5,†]

[1]*Quy Nhon University, 170 An Duong Vuong, Quy Nhon, Binh Dinh*

[2]*Duy Tan University, 03 Quang Trung, Hai Chau, Da Nang*

[3]*Posts and Telecommunications Institute of Technology, Km 10 Nguyen Trai, Thanh Xuan, Hanoi*

[4]*Institute of Materials Science, 18 Hoang Quoc Viet, Cau Giay, Hanoi*

[5]*Institute of Physics, 10 Dao Tan, Ba Dinh, Hanoi*

[†]*E-mail:* thanhnt@ims.vast.ac.vn; nxnghia@iop.vast.vn

Received 16 May 2019
Accepted for publication 14 May 2020
Published 19 May 2020

Abstract. *With the advantages of selectivity, spectral resolution and reduction of interference on account of light scattering, synchronous luminescence spectroscopy is successfully applied to analyze complex mixtures with overlapped emission and/or excitation spectra. Herein, we report the application of synchronous luminescence spectroscopy to detect luminescence centers in colloidal $Cd_{0.3}Zn_{0.7}S$ nanocrystals and the emission peaks at 460 and 515 nm which are attributed to the emission transitions related to sulfur and zinc/cadmium vacancies. The obtained results are useful to clarify the nature of luminescence centers as well as relaxation mechanism in $Cd_xZn_{1-x}S$ nanocrystals.*

Keywords: Colloidal $Cd_{0.3}Zn_{0.7}S$ nanocrystals, Synchronous luminescence spectroscopy, Luminescence centers.

Classification numbers: 78.67.Bf, 78.55.Et, 81.07.Bc.

I. INTRODUCTION

Photoluminescence (PL) measurements yield information about the energetic positions of the electronic states in the band gap of semiconductors. Such localized states can be due to various types of structural imperfections like vacancies, interstitial atoms, and atoms at surfaces and grain boundaries. The imperfections can create either donor or acceptor levels in the band gap, and it is often difficult to determine their exact energy positions because the donor or acceptor levels may be very close in energy and cannot be resolved in the luminescence bands [1-3]. It is possible that a significant narrowing of emission peaks is achieved by using synchronous luminescence spectroscopy (SLS) [4]. In the conventional PL spectroscopy, the spectrum is obtained by scanning the emission wavelength (λ_{emiss}) under the photoexcitation at a chosen wavelength (λ_{exc}). The experiment by SLS is performed by varying synchronously both the photoexcitation λ_{exc} and emission λ_{emiss} wavelengths at a constant difference $\Delta\lambda = \lambda_{emiss} - \lambda_{exc}$.

Recently, SLS was successfully applied for size dependent simultaneous analysis of CdTe nanocrystals (NCs) and their mixtures [5], to study the midgap electronic states in nanocrystalline SrTiO3 [6], $CaTiO_3$ [7], anatase and rutile TiO_2 [8,9]. Herein, we report the application of SLS to detect luminescence centers in homogeneous $Cd_{0.3}Zn_{0.7}S$ NCs prepared by wet chemical method.

II. EXPERIMENT

Synthesis and purification of $Cd_{0.3}Zn_{0.7}S$ NCs

Initial chemicals, including zinc stearate (Zn(St)2, 98%), cadmium oxide (CdO, 99.99%, powder), sulfur (S, 99.98%, flour), 1-octadecene (ODE, 90%), and stearic acid (SA, 90%), were purchased from Aldrich and used as received without further purification.

For the synthesis of $Cd_{0.3}Zn_{0.7}S$ NCs, a mixture of S (1 mmol) and ODE (24 mmol) was stirred at 100˚C for 60 min in a vessel. Meanwhile, 0.3 mmol of CdO, 1.4 mmol of SA, and 60 mmol of ODE were put in a three-neck flask, which was then heated up to 280˚C for 60 min in order to form a transparent Cd solution. Zn solution was obtained by dissolving 0.7 mmol of $Zn(St)_2$ in mixture of SA (0.036 mmol) and ODE (60 mmol) at 180 ^{o}C for 60 min. After that, S precursor solution was swiftly injected into a reaction flask containing a half of Zn and Cd precursor solutions at 280 ^{o}C. Small amounts of remaining Zn and Cd precursor solutions then were alternately injected into reaction flask. The NC sample was prepared with reaction time of 270 min. The precursor solutions and NCs are prepared under the condition of the nitrogen flow. For simplicity of presentation, the calculated Cd and Zn contents (0.3 and 0.7, respectively) will be used in the chemical formula of the sample.

Crude solution obtained after preparing NC sample was mixed with isopropanol (according to the ratio of 1/3 in volume). NCs were collected by using a centrifuge, which worked with speed of 15000 rpm for 3 min. After purification, a part of the product in powder was used to investigate crystal structure. Other parts were dispersed in toluene for checking morphology, size and spectroscopic measurements.

Measurements

Transmission electron microscopy (TEM) image of $Cd_{0.3}Zn_{0.7}S$ sample was recorded using JEM 1010 microscope (Jeol). The sample was mounted on a carbon-coated cooper-mesh grid. X-ray diffraction (XRD) pattern was obtained from an X-ray diffractometer (Siemens, D5005), using

a Cu K_α radiation source with λ = 1.5406 Å. Optical absorption spectrum was recorded with a Jasco 670 spectrometer.

The PL spectrum was collected using Fluorolog FL3-22 spectrometer (Horiba Jobin Yvon). This instrument is equipped with dual monochromator gratings on the excitation and emission light paths. To minimize optical artifacts due to primary and secondary absorption of light in solid specimen, the PL spectrum was obtained in the Front Face (FF) geometry. To eliminate the consequences of fluctuations of intensity of the photoexcitation source, the emission signal S from the sample was divided by the reference signal R generated by the excitation beam before reaching the sample, and the (S/R) ratio was always used as an Y axis of the spectrum. The PL emission spectrum was recorded with excitation and emission slits at 5 nm.

SLS measurement was conducted using the same Fluorolog FL3-22 spectrometer in the FF geometry as described above. The (S/R) ratio was used to construct the Y axis of all synchronous luminescence spectra, and the sample was in the same physical form as in conventional PL measurement. The $\Delta\lambda$ parameter was varied at the 10 nm increments. Synchronous luminescence spectra were also recorded with excitation and emission slits set at 5 nm.

III. RESULTS AND DISCUSSION

Figure 1 shows the TEM image of $Cd_{0.3}Zn_{0.7}S$ NCs. They have dot-like shape with the average diameter of $\sim$ 4.5 nm and narrow size distribution.

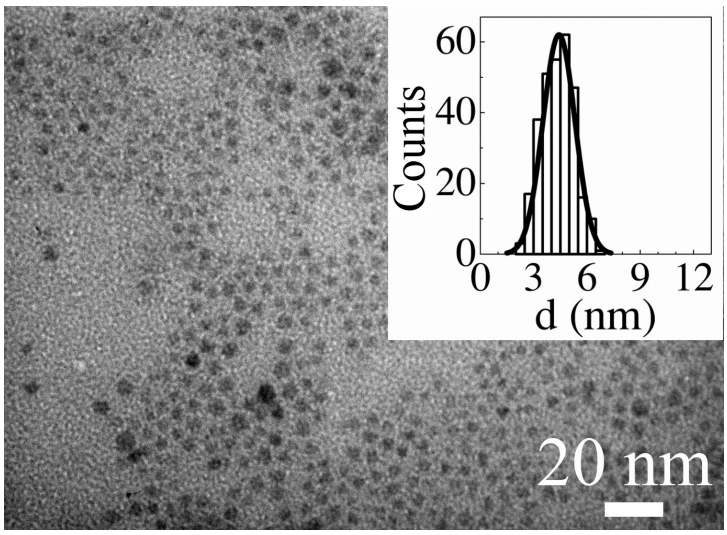

Fig. 1. TEM image and size distribution of $Cd_{0.3}Zn_{0.7}S$ NCs.

XRD pattern of $Cd_{0.3}Zn_{0.7}S$ sample is shown in Fig. 2(a). The shoulders on both sides of diffraction peak centered at about 27.5° reveal the superposition of diffraction peaks of zinc blende (Zb) and wurtzite (Wz) phases in $Cd_{0.3}Zn_{0.7}S$ NCs. To separate the diffraction peaks corresponding to Zb and Wz phases, Rietveld refinement analysis was performed using FullProf program modified with atomic scattering factors for electrons (Wz in space group $P6_3mc$ and Zb in space group $F-43m$) [10–12].

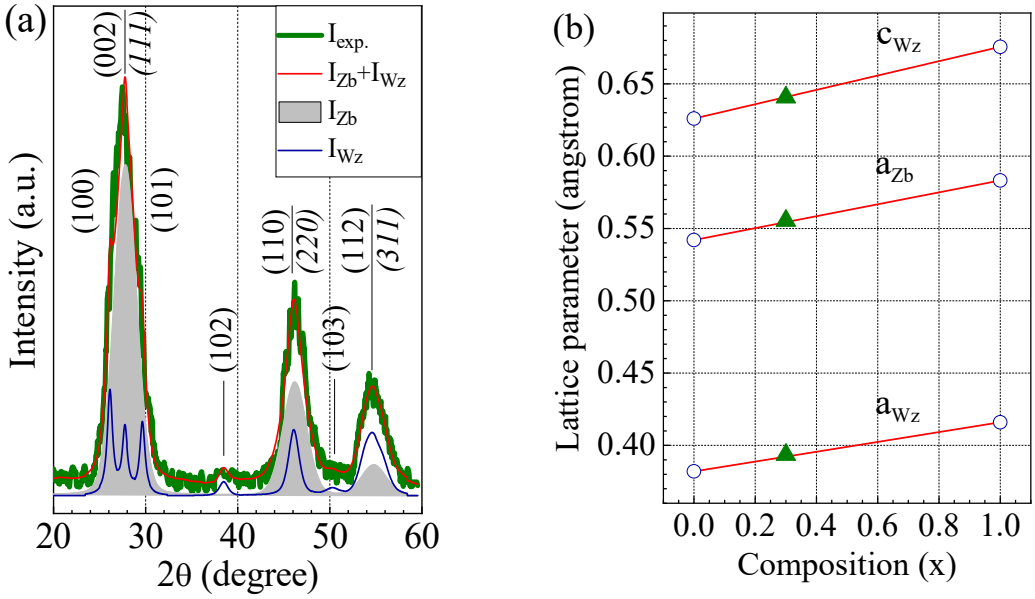

Fig. 2. (a) Rietveld refinement analysis of XRD pattern, and (b) the evidence on homogeneous alloying of $Cd_{0.3}Zn_{0.7}S$ NCs. The Miller indices of Zb phase are shown by italic numbers in parentheses.

The Zb phase of $Cd_{0.3}Zn_{0.7}S$ NCs is characterized by the diffraction peaks centered at 27.8, 46.2 and 54.8 ° corresponding to the Miller indices (111), (220) and (311), respectively. Meanwhile, the remaining part of XRD pattern indicates the Wz phase with the diffraction peaks centered at 26.1, 27.7, 29.6, 38.5, 46.1, 50.3 and 54.7 °, which correspond to the Miller indices (100), (002), (101), (102), (110), (103) and (112), respectively. As displayed in Fig. 2(b), the obtained lattice parameters of Zb and Wz phases are in good agreement with the lattice parameters of bulk $Cd_{0.3}Zn_{0.7}S$ material, determined based on Vegard's law [13, 14]. This confirms the homogeneous alloying of $Cd_{0.3}Zn_{0.7}S$ NCs. Moreover, the Zb phase fraction calculated basing on the integrated intensities of diffraction peaks of Wz and Zb phases is $\sim 73\%$. It should be noted that, beside the native defects of $Cd_xZn_{1-x}S$ material, the interface regions between the different structural phases usually contain the additional lattice defects, these may dominate the optical spectrum.

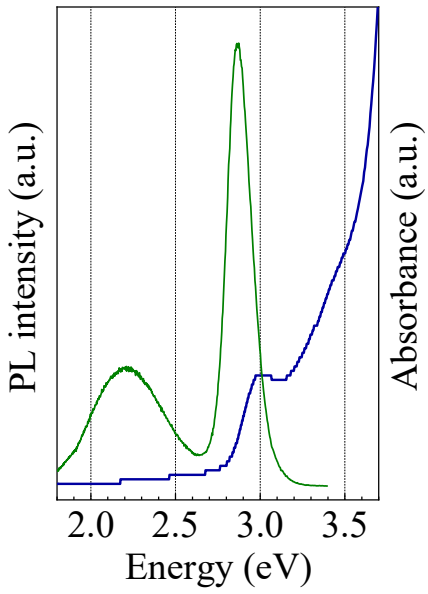

Fig. 3. Absorption and PL spectra of $Cd_{0.3}Zn_{0.7}$ S NCs.

The absorption and PL spectra of $Cd_{0.3}Zn_{0.7}S$ NCs are depicted in Fig. 3. The optical band gap energy of $Cd_{0.3}Zn_{0.7}S$ NCs is determined at the position of first absorption peak and has value of 3.02 eV. Since the optical band gap energies of Zb and Wz phases are different [15, 16], the coexistence of both these structural phases in same NC leads to convolution of their absorption spectra. Based on the equation for nonlinear dependence of the optical band gap energy of $Cd_xZn_{1-x}S$ NCs on the composition and particle radius [17, 18], it can be deduced that 3.02 eV is the value of the optical band gap energy of the investigated sample. Simultaneously, the peak at 3.02 eV is attributed to the absorption transition of Zb phase because the Zb phase fraction is about 2.7 times larger than the Wz phase one. It also means that the absorption spectrum of Wz phase is covered by that of Zb phase. Remarkably, the absorption spectrum of $Cd_{0.3}Zn_{0.7}S$ NCs has a tail in the low energy region. This tail is originated by absorption transitions from valence band to the localized states, from the localized states to conduction band, and between the localized states [19–21], which have smaller energy in comparison to the optical band gap energy. In other words, the appearance of the absorption tail is related not only to the surface states, but also to the native defects as well as the additional defects in the interface region between the Zb and Wz phases of $Cd_{0.3}Zn_{0.7}S$ NCs. The PL spectrum of $Cd_{0.3}Zn_{0.7}S$ NCs consists of a strong peak at 2.86 eV (433 nm) and broad emission band centered at 2.2 eV (563 nm). The full width at half maximum of high energy peak is 0.2 eV (23 nm), exhibiting the narrow size distribution of $Cd_{0.3}Zn_{0.7}S$ sample.

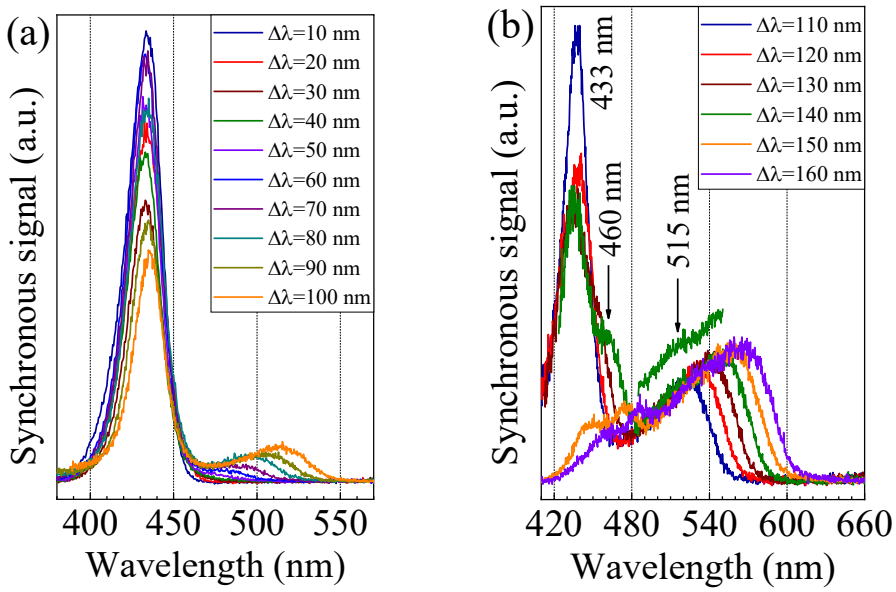

Fig. 4. (Color online) Synchronous luminescence spectra at $\Delta\lambda$ parameter of: (a) 10-100 nm; and (b) 110-160 nm. To more clearly identify the peak at 515 nm, the range of 490-550 nm of the spectrum with $\Delta\lambda = 140$ nm is shown in Fig. 4(b).

Figure 4 shows synchronous luminescence spectra at variable $\Delta\lambda$ parameter. As can be seen in Fig. 4(b), large values of $\Delta\lambda > 100$ nm are suitable for detection of luminescence centers.

Differently from Fig. 4(a), two spectral shoulders at 460 nm (2.69 eV) and 515 nm (2.41 eV) are clearly observed at $\Delta\lambda$ = 140 nm. The shoulder at λ_{emiss} = 460 nm originates from photoexcitation at $\lambda_{exc} = \lambda_{emiss} - \Delta\lambda$ = 460 nm - 140 nm = 320 nm (3.87 eV). Similarly, the shoulder at λ_{emiss} = 515 nm originates from photoexcitation at λ_{exc} = 375 nm (3.31 eV). Because the optical band gap energy of $Cd_{0.3}Zn_{0.7}S$ NCs is 3.02 eV, both two spectral shoulders at 460 and 515 nm originate from the photoexcitation across the direct band gap in NCs.

The PL spectra of $Cd_xZn_{1-x}S$ ($0 \leq x \leq 1$) NCs may contain peaks due to self-trapped exciton, sulfur vacancy (denoted V_S), zinc/cadmium vacancy (V_{Zn}/V_{Cd}), interstitial sulfur (I_S), interstitial zinc/cadmium (I_{Zn}/I_{Cd}), and surface states. Based on the positions of absorption and emission peaks in Fig. 3, the emission peak centered at 433 nm is attributed to exciton recombination. The emission peak at 460 nm is due to the recombination of carriers between sulfur vacancy V_S related donor level and the valence band edge, and the emission peak at 515 nm can be attributed to the radiative transition from zinc/cadmium interstitial I_{Zn}/I_{Cd} related donor level to zinc/cadmium vacancy V_{Zn}/V_{Cd} related acceptor level [3, 22, 23] (see Fig. 5).

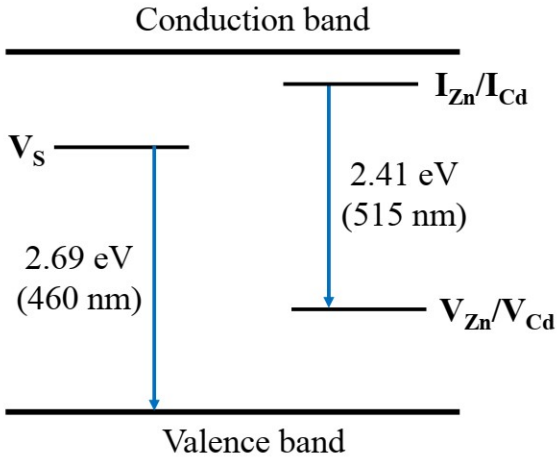

Fig. 5. Energy level diagram of 460 nm and 515 nm radiative transitions in $Cd_{0.3}Zn_{0.7}S$ NCs.

IV. CONCLUSION

Synchronous luminescence spectra are superior to conventional PL spectra in resolving characteristic emission peaks of homogeneous $Cd_{0.3}Zn_{0.7}S$ NCs. Beside the emission peak at 433 nm due to the exciton recombination and luminescence related with the surface states, two spectral shoulders at 460 and 515 nm have been detected by synchronous luminescence measurement. The 460 nm shoulder is attributed to the recombination of carriers between sulfur vacancy related donor level and the valence band edge. Meanwhile, the 515 nm shoulder is originated due to the radiative recombination from zinc/cadmium interstitial related donor level to zinc/cadmium vacancy related acceptor level. The obtained results are useful to clarify the nature of luminescence centers as well as relaxation mechanism in $Cd_xZn_{1-x}S$ NCs.

ACKNOWLEDGMENTS

This research is funded by Vietnam National Foundation for Science and Technology Development (NAFOSTED) under grant number 103.02-2017.54.

REFERENCES

[1] D. Denzler, M. Olschewski, and K. Sattler, *J. Appl. Phys.* **84** (1998) 2841.
[2] J. R. Lakowicz, *Principles of Fluorescence Spectroscopy*, third ed., Springer, 2006.
[3] M. A. Osman, and A. G. Abd-Elrahim, *Opt. Mater.* **77** (2018) 1.
[4] T. Vo-Dinh, *Anal. Chem.* **50** (1978) 396.
[5] D. Patra, and T. H. Ghaddar, *Talanta* **77** (2009) 1549.
[6] S. Taylor, and A. Samokhvalov, *Spectrochimica Acta Part A: Molecular and Biomolecular Spectroscopy* vol. **174** (2017) 54.
[7] A. Alzahrani, and A. Samokhvalov, *J. Porous Mater.* **24** (2017) 1145.
[8] A. Samokhvalov, *J. Lumin.* vol **192** (2017) 388.
[9] A. Samokhvalov, *J. Phys. Chem. C* vol. **121** (2017) 21985.
[10] V. Kumar, S. Kumari, P. Kumar, M. Kar, and L. Kumar, *Adv. Mater. Lett.* **6** (2015) 139.
[11] J. Li, B. Kempken, V. Dzhagan, D.R.T. Zahn, J. Grzelak, S. Mackowski, J. Parisi, and J. Kolny-Olesiak, *CrystEngComm* **17** (2015) 5634.
[12] S. Sain, and S.K. Pradhan, *J. Alloy Compd.* **509** (2011) 4176.
[13] A. K. Chawla, S. Singhal, S. Nagar, H. Gupta, and R. Chandra, *J. Appl. Phys.* **108** (2010) 123519.
[14] H. Alehdaghi, M. Marandi, M. Molaei, A. Irajizad, N. Taghavinia, H. Alehdaghi, M. Marandi, M. Molaei, A. Irajizad, and N. Taghavinia, *J. Alloys Compd*. **586** (2014) 380.
[15] J. Li, and L.W . Wang, *Nano Lett.* **3** (2003) 1357.
[16] J. Jasieniak, C. Bullen, J. V. Embden, and P. Mulvaney *J. Phys. Chem. B* **109** (2005) 20665.
[17] A.K. Chawla, S. Singhal, S. Nagar, H. Gupta, and R. Chandra, *J. Appl. Phys.* **108** (2010) 123519.
[18] J. Kim, J. Lee, H.S. Jang, D.Y. Jeon, and H. Yang, *J. Nanosci. Nanotechnol.* **11** (2011) 725.
[19] J. Yang, Y.Q. Gao, J. Wu, Z.M. Huang, X.J. Meng, M.R. Shen, J.L. Sun, and J.H. Chu, *J. Appl. Phys.* **108** (2010) 114102.
[20] B. Choudhury, B. Borah, and A. Choudhury, *Photochem. Photobiol.* **88** (2012) 257.
[21] P. Guyot-Sionnest, E. Lhuillier, and H. Liu, *J. Chem. Phys.* **137** (2012) 154704.
[22] J. Manam, V. Chattejee, S. Das, A. Choubey, and S.K. Sharma, *J. Lumin.* **130** (2010) 292.
[23] P.K. Narayanam, P. Soni, R.S. Srinivasa, S.S. Talwar, and S.S. Major, *J. Phys. Chem. C* **117** (2013) 4314.